Single-inclusive production of large-p_T charged particles in hadronic collisions at TeV energies and perturbative QCD predictions

François Arleo,[a] **David d'Enterria**[b] **and Andre S. Yoon**[c]

[a]*LAPTH*[1]*, Université de Savoie,*
  CNRS, BP 110, 74941 Annecy-le-Vieux cedex, France

[b]*ICREA & Institut Ciències del Cosmos, Univ. Barcelona,*
  08028 Barcelona, Catalonia

[c]*Laboratory for Nuclear Science, MIT,*
  Cambridge, MA 02139-4307, U.S.A.

  E-mail: arleo@lapp.in2p3.fr, david.d'enterria@cern.ch, y_alive@mit.edu

ABSTRACT: The single inclusive spectrum of charged particles with transverse momenta $p_T = 3 - 150$ GeV/c measured at midrapidity by the CDF experiment in proton-antiproton (p-$\bar{p}$) collisions at $\sqrt{s} = 1.96$ TeV is compared to next-to-leading order (NLO) perturbative QCD calculations using the most recent parametrizations of the parton distributions and parton-to-hadron fragmentation functions. Above $p_T \approx 20$ GeV/c, there is a very sizeable disagreement of the Tevatron data compared to the NLO predictions and to x_T-scaling expectations, suggesting a problem in the experimental data. We also present the predictions for the p_T-differential charged hadron spectra and the associated theoretical uncertainties for proton-proton (p-p) collisions at LHC energies ($\sqrt{s} = 0.9$–14 TeV). Two procedures to estimate the charged hadron spectra at LHC heavy-ion collision energies ($\sqrt{s} = 2.76$, 5.5 TeV) from p-p measurements are suggested.

---

[1]Laboratoire d'Annecy-le-Vieux de Physique Théorique, UMR5108.

Contents

1 Introduction

Hadron production at large transverse momenta ($p_{_T} \gg \Lambda_{\rm QCD} \approx 0.2\,{\rm GeV}$) in hadronic interactions originates from the fragmentation of the hard scattered partons produced in the collision. The presence of a hard scale in the process allows one to employ the powerful theoretical machinery of collinear factorisation [1] to compute the corresponding production cross sections. High-$p_{_T}$ hadron cross sections can be thus obtained as a convolution of (i) long-distance universal pieces representing the structure of the initial hadrons (parton distribution functions, PDFs) as well as the fragmentation of a final-state quark or gluon into the observed hadron (fragmentation functions, FFs), and (ii) short-distance parts that describe the hard partonic interactions calculable as a perturbative expansion in terms of the strong running coupling $\alpha_{_S}$. The measurement of high-$p_{_T}$ hadroproduction in p-p and p-$\bar{p}$ collisions provides, thus, a valuable testing ground of the perturbative regime of Quantum Chromodynamics (pQCD) and of the non-perturbative objects (PDFs, FFs) needed to compute a large variety of cross sections at hadronic colliders.

Theoretically, lowest-order (LO) calculations of the inclusive hadron cross sections were performed in the late 70s [2], later improved at next-to-leading order (NLO) [3–5] and more recently at next-to-leading-log (including soft gluon resummation) [6–8] accuracies. The latest phenomenological developments in this field have focused on constraints of the proton PDFs (in particular the polarised ones [8, 9]), on improvements of the parton-to-hadron (in

– 1 –

particular, gluon-to-hadron) FFs [10, 11], as well as on baseline measurements of relevance for high-energy heavy-ions collisions [12]. On the experimental side, inclusive unidentified charged hadron production — i.e. $pp, p\bar{p} \to h^\pm X$, where $h^\pm = (h^+ + h^-)$ is effectively the sum of pions (about 60% of all hadrons), kaons (about 20% of the total) and protons (about 10% of all hadrons) and their antiparticles — have been measured above $p_T \approx 1$ GeV/c at the ISR ($\sqrt{s} = 31$, 44, 63 GeV) [13, 14], at RHIC ($\sqrt{s} = 200$ GeV) [15, 16], Sp$\bar{p}$S ($\sqrt{s} = 0.2$, 0.5, 0.9 TeV) [17], and Tevatron ($\sqrt{s} = 0.63$, 1.8, 1.96 TeV) [18–20] energies. Except at Tevatron, the rest of measurements are unfortunately in a moderate p_T range ($p_T \approx 12$ GeV/c at most). The latest comparisons of the available charged hadron spectra, at RHIC energies [9, 15, 16], to NLO calculations [6, 7] show a good data-theory agreement above $p_T \approx 1.5$ GeV/c for central and forward rapidities [12].

In this paper, we compare NLO pQCD calculations to the latest charged particle spectrum measured at Tevatron and we present predictions with their theoretical uncertainties for the high-p_T hadron spectra expected at LHC energies. The motivation is two-fold. First, the most recent CDF charged particle spectrum [20] covers a very large p_T range, up to $p_T = 150$ GeV/c where pQCD predictions are reliable and can be confronted to the data. Similarly, comparable "minimum bias" measurements are expected to be available in the early running of the LHC [21–23]. CMS has already measured a first, yet mostly low-p_T, charged hadron spectrum at $\sqrt{s} = 2.36$ TeV [24]. Secondly, at the LHC, a p-p reference hadron spectrum will be needed at the *same* centre-of-mass (c.m.) energy as that of heavy-ion (Pb-Pb) collisions to study the high-p_T suppression observed in nucleus-nucleus reactions at RHIC [25, 26]. Since the Pb-Pb results will be nominally obtained at $\sqrt{s_{NN}} = 5.5$ TeV a pQCD-based interpolation between the results recorded at Tevatron ($\sqrt{s} = 1.96$ TeV) and during the first LHC p-p run ($\sqrt{s} = 7$ TeV) will be needed.

The paper is organized as follows. In section 2 we succinctly remind the theoretical framework of our study based on the next-to-leading-order pQCD Monte Carlo (MC) code INCNLO [27, 28]. In section 3, we compare the charged particle spectra measured at mid-rapidity in p-$\bar{p}$ collisions at $\sqrt{s} = 1.96$ TeV [20] to the NLO calculations INCNLO and to the LO parton shower MC PYTHIA, as well as to simple x_T-scaling expectations. We find that the *maximum* theoretical uncertainties of the NLO prediction — associated to the PDF, FF and scale variations added in quadrature — are $\pm 40\%$. For increasing transverse momenta, the data is a factor up to 3 orders of magnitude larger than the perturbative predictions. We conclude that above $p_T \approx 20$ GeV/c, there is no possibility to accommodate the data-theory discrepancy even accounting for possible additional contributions to the charged particle yield coming e.g. from heavy-quarks or vector-boson (plus jet) production. The fact that the parent jet p_T-differential spectrum is, on the contrary, well reproduced by NLO calculations and that the single particle data also violate simple x_T-scaling expectations, suggest a problem in the experimental results at the highest p_T values. Finally, in section 4 we present the charged hadron spectra and associated uncertainties predicted by INCNLO in p-p collisions in the range of energies covered by the LHC ($\sqrt{s} = 0.9 - 14$ TeV), and propose two methods to determine the p-p spectra at intermediate LHC energies of relevance for heavy-ion running.

2 Hadroproduction in factorised pQCD

The inclusive cross section for the production of a single hadron, differential in transverse momentum p_T and rapidity y, takes the following form at next-to-leading order in α_S [29]:

$$\frac{\mathrm{d}\sigma}{\mathrm{d}\mathbf{p_T}\mathrm{d}y} = \sum_{i,j,k=q,g} \int \mathrm{d}x_1 \ \mathrm{d}x_2 \ F_{i/p}(x_1,\mu_F) \ F_{j/p}(x_2,\mu_F) \ \frac{\mathrm{d}z}{z^2} \ D_k^h(z,\mu_{FF})$$
$$\times \left[\left(\frac{\alpha_S(\mu_R)}{2\pi}\right)^2 \frac{\mathrm{d}\widehat{\sigma}_{ij,k}}{\mathrm{d}\mathbf{p_T}\mathrm{d}y} + \left(\frac{\alpha_S(\mu_R)}{2\pi}\right)^3 K_{ij,k}(\mu_R,\mu_F,\mu_{FF}) \right]. \quad (2.1)$$

Here $F_{i/p}(x_1,\mu_F)$ are the PDFs of the incoming protons p at parton momentum fraction x, $D_k^h(z,\mu_{FF})$ are the parton-to-hadron FFs describing the transition of the parton k into an unidentified hadron h carrying a fraction z of its momentum, $\mathrm{d}\widehat{\sigma}_{ij,k}/\mathrm{d}\mathbf{p_T}\mathrm{d}y$ is the Born cross section of the subprocess $i + j \rightarrow k + \mathrm{X}$, and $K_{ij,k}$ is the corresponding higher-order term (the full kinematic dependence is omitted for clarity). In this paper, we use the INCNLO programme [27, 28] to compute the cross sections, supplemented with various PDFs and FFs sets (see below). The truncation of the perturbative series at next-to-leading order accuracy in α_S introduces an artificial dependence with magnitude $\mathcal{O}\left(\alpha_S{}^3\right)$, of the cross section on initial-state (μ_F) and final-state (μ_{FF}) factorization scales, as well as on the renormalization scale μ_R. The choice of scales is arbitrary but the standard procedure is to choose a value around the natural physical scale of the hard scattering process, here given by the p_T of the produced hadron. We consider below scale variations $\mu_R, \mu_F, \mu_{FF} = \kappa\, p_T$, with $\kappa = 0.5 - 2$ to gauge the theoretical uncertainty linked to the neglected higher-order terms. Hereafter, whenever the scales μ_R, μ_F and μ_{FF}, are given a common value, the latter is denoted μ.

The two non-perturbative inputs of eq. (2.1) are the parton densities and the fragmentation functions. The former are mostly obtained from global-fit analyses of HERA proton structure function data, the latter from hadron production results in e^+e^- collisions. We use here the three latest PDFs parametrisations available: CTEQ6.6 [30], MSTW08 [31, 32] and NNPDF1.2 [33], included in the LHAPDF (version 5.7.1) package [34], which take into account the most up-to-date data from deep-inelastic lepton-proton scattering and hadronic collisions as well as various theoretical improvements. For the fragmentation functions into hadrons, we use and compare the three more recent FF sets available: DSS [35], AKK08 [36] and HKNS [37], which, except for the latter, include for the first time also hadron-hadron collision data in their global analyses. These new FF fits cover a larger z range and are more sensitive to the gluon fragmentation which dominates high-p_T hadron production in p-p collisions [10, 11].

For transverse momenta close to the phase space boundary where the p_T of the hadron is about half of the partonic centre-of-mass energy ($x_T = 2p_T/\sqrt{s} \approx 0.1 - 1$), the coefficients of the perturbative expansion are enhanced by extra powers of logarithmic terms of the form $\alpha_S{}^n \ln^{2n-1}(1-x_T)/(1-x_T)$ [38–40]. Resummation to all orders of such "threshold" terms — which appear when the initial partons have just enough energy to produce the high-p_T hadron — have been carried out at next-to-leading logarithmic (NLL) accuracy

in [6–8]. Interestingly, the NLL results provide a much reduced scale-dependence than the NLO approximation. The presently used fixed-order calculations (INCNLO) do not include threshold resummations but their effect in the final spectrum is expected to be less important since the typical charged hadron p_T range covered by the Tevatron and LHC experiments, $x_T \equiv 2p_T/\sqrt{s} \approx 10^{-4} - 10^{-1}$, is far away from the region where such effects start to play a role.

3 Tevatron data versus perturbative QCD

In this section we compare the high-p_T charged particle spectrum measured by the CDF collaboration [20] in the pseudorapidity range $|\eta| < 1$ to the predictions of INCNLO [27, 28] and PYTHIA [41] MCs and to simple perturbative expectations based on x_T-scaling [42–45]. The measured spectrum covers the range $p_T = 0.4 - 150$ GeV/c, but a comparison to pQCD predictions is only meaningful at high enough p_T; therefore we impose a minimal cut of $p_T = 3$ GeV/c. For the NLO analysis, we study separately the effects on the spectrum of varying in the calculations the three theoretical scales ($\mu = p_T/2, p_T, 2p_T$), PDFs (MSTW08, CTEQ6.6 and NNPDF1.2) and FFs (AKK08, DSS and HKNS). We use PYTHIA to determine possible extra contributions to the measured high-p_T tracks spectrum coming from heavy-quark fragmentation as well as from real and virtual vector-boson production, either single-inclusive or in association with a jet.

3.1 Data versus INCNLO

The measured CDF charged particle p-$\bar{p}$ single inclusive distribution is compared to the INCNLO predictions for charged hadrons in figure 1. First, we note that the measured primary track spectrum is not corrected for contributions from charged particles other than hadrons. Possible contaminations from stable leptons (electrons, positrons and muons) are not in principle removed from the measured spectrum. As we discuss *a posteriori* in section 3.2, those amount however only to a small fraction (a few percents) of the total charged particle tracks coming from quark and gluon jet fragmentation according to our PYTHIA simulations. The INCNLO prediction shown in figure 1 is that which best fits the (low p_T range of) the experimental results. We see that below $p_T \approx 20$ GeV/c data and theory agree well for the choice of scales $\mu = 2p_T$, CTEQ6.6 parton densities, and AKK08 parton-to-hadron fragmentation functions. Above this p_T value, the CDF spectrum starts to rapidly deviate from the theoretical predictions. At the highest transverse momenta the data is up to a factor 800 above the NLO calculations. A very conservative quadratic sum of all uncertainties discussed hereafter — amounting to $\pm 30\%$ for the scales, $\pm 10\%$ for the PDFs, and $\pm 25\%$ for the FFs choices — would result in a maximum theoretical uncertainty of $\pm 40\%$ in the yields (dashed lines around the data/theory ratio).

Scale uncertainty: first, in the INCNLO calculations we have fixed the PDFs and FFs to the CTEQ6.6 and DSS sets respectively,[1] and computed the corresponding spectra

---

[1]The choice is in principle arbitrary, other PDF and FF combinations yield similar results for the scale dependence.
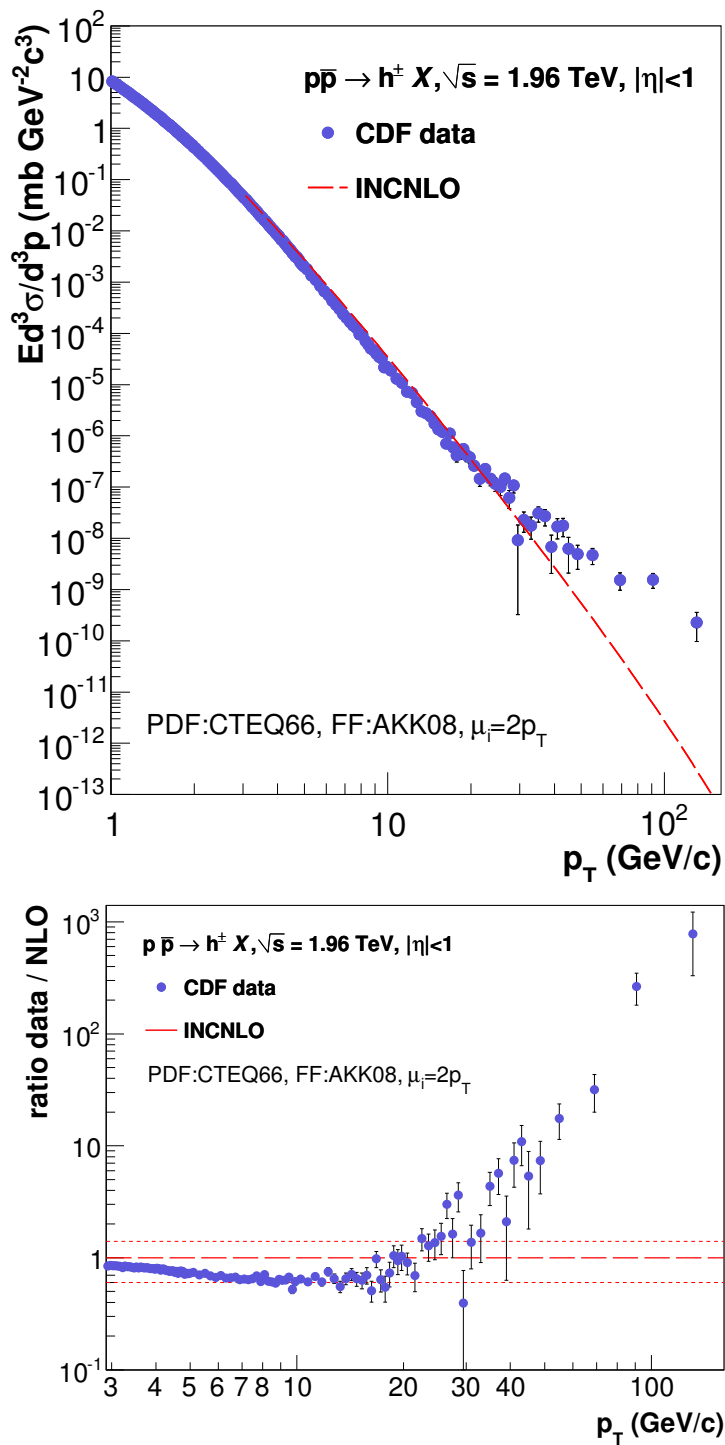
Figure 1. Top: Comparison of the charged particle p_T spectrum measured by CDF in p-$\bar{p}$ collisions at $\sqrt{s} = 1.96\,\mathrm{TeV}$ [20] to NLO pQCD predictions with PDFs fixed to CTEQ6.6, scales to $\mu = 2p_T$, and FFs to AKK08. Bottom: Corresponding ratio of CDF data over theory. The dashed lines indicate the maximum $\pm 40\%$ theoretical uncertainty of the calculations (see text).
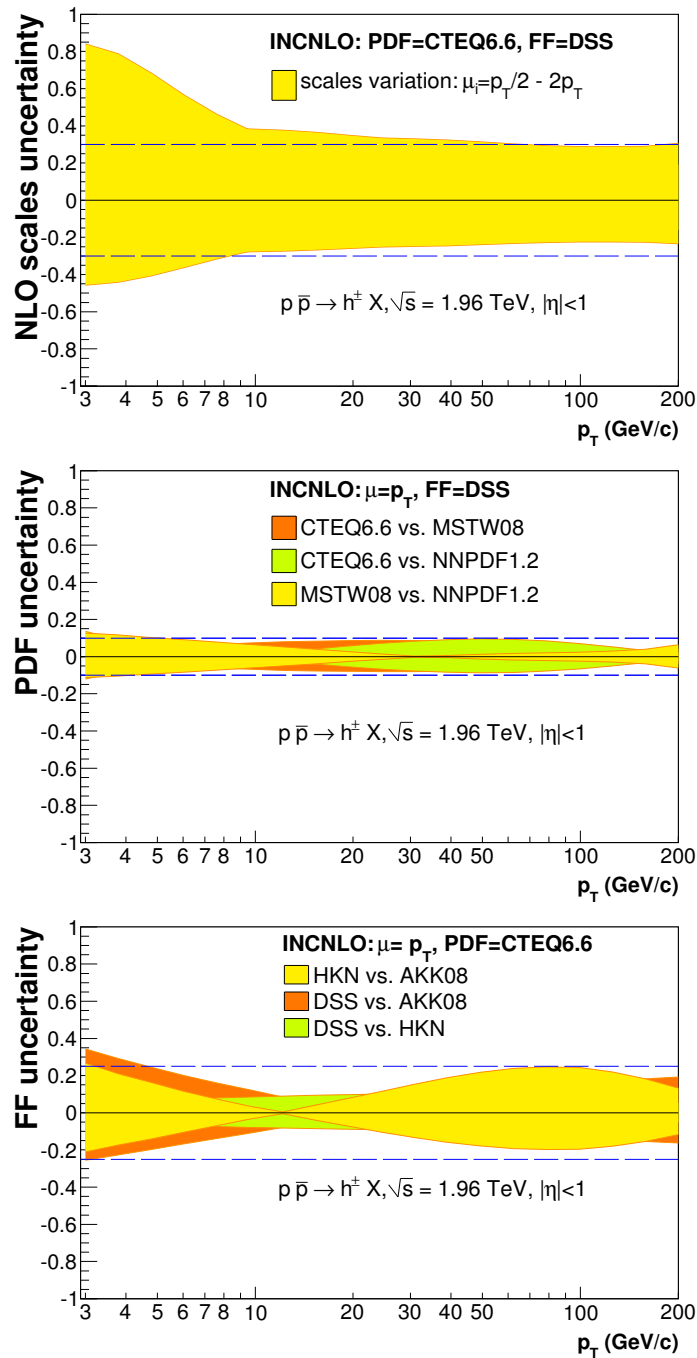
Figure 2. Fractional differences between the INCNLO charged hadron spectra in p-$\bar{p}$ at $\sqrt{s} = 1.96\,\text{TeV}$ for varying scales μ_i, PDF and FF. Top: Scale uncertainty obtained for fixed PDF (CTEQ6.6) and FF (DSS) varying all three scales within $\mu_i = p_T/2 - 2p_T$ (the dashed lines indicate a $\pm30\%$ uncertainty). Middle: PDF uncertainty obtained for fixed $\mu = p_T$ and FF (DSS) with three PDFs: CTEQ6.6, MSTW08, NNPDF1.2 (the dashed lines indicate $\pm10\%$ differences). Bottom: FF uncertainty obtained for fixed scales ($\mu = p_T$) and PDF (CTEQ6.6) with three FFs: AKK08, DSS, HKNS (the dashed lines represent $\pm25\%$).

setting the three theoretical scales to three different values $\mu_{F,M,FF} = p_T/2, p_T, 2p_T$ in all possible 27 combinations. The corresponding range of predictions is shown in figure 2 (top) where we plot a shaded band covering the whole range of fractional differences between the spectra obtained for any choice of scales. The "closest-to-the-average" spectrum is obtained setting all scales to $\mu = p_T$. The largest (resp. lowest) charged hadron yield predictions are obtained with mostly all three scale values set to $\mu_i = p_T/2$ (resp. $\mu_i = 2p_T$). At low p_T the scale uncertainty is quite large (indicating as expected larger higher-order corrections) but otherwise above $p_T = 10$ GeV/c it stays roughly constant at around $\pm 30\%$ up to the highest momenta considered (dashed lines in the figure).

PDF uncertainty: second, in the middle panel of figure 2 we show as a function of p_T the theoretical uncertainty associated to the PDF choice. It has been obtained with INCNLO comparing the fractional differences between the single charged hadron spectra at $\sqrt{s} = 1.96$ TeV for fixed scales ($\mu = p_T$) and FF (DSS) and three different PDFs. The dashed bands plotted cover the range of maximum relative differences in the theoretical spectra obtained with MSTW08, CTEQ6.6 and NNPDF1.2. Those differences are small, below 10% and mostly p_T-independent (dashed lines).

FF uncertainty: last, we have used INCNLO complemented with the three latest FFs available in the market: AKK08, DSS and HKNS, to compute the charged hadron spectrum for the CDF kinematics, with scales ($\mu = p_T$) and PDFs (CTEQ6.6) fixed. The main differences between FF sets concern the fractional $\pi^\pm$, $K^\pm$ and $p/\bar{p}$ compositions as a function of p_T. Yet, the total[2] hadron yield predicted by the three FFs for p-$\bar{p}$ at 1.96 TeV is quite similar as can be seen in the bottom panel of figure 2 where we plot the relative differences between the spectra computed for varying FFs. The maximum theoretical uncertainty linked to the FF choice amounts to about $\pm 25\%$ of the charged hadron yield at any p_T (dashed lines), although the differences between FFs appear to be smaller at intermediate hadron $p_T \approx 10 - 25$ GeV/c.

A conservative quadratic sum of the fractional uncertainties linked to the NLO scales, PDFs and FFs choices results in a total theoretical uncertainty of order $\pm 40\%$ whereas the maximum difference between the data and the calculations amounts to much larger factors, up to $\mathcal{O}(10^3)$ at $p_T \gtrsim 100$ GeV/c (figure 1).

3.2 Data versus PYTHIA

Given the large discrepancy between the experimental and NLO predictions for the charged particle spectrum at high-p_T one may wonder whether other charged particles — apart from $\pi^\pm, K^\pm, p/\bar{p}$ coming from the fragmentation of quarks and gluons — may contribute in any way to the experimentally measured distribution beyond $p_T \approx 20$ GeV/c. A first possibility that we have considered is whether other charged products from charm and bottom jets (with relative increasing importance at large transverse momentum) play any

---

[2]As a cross check, for all FF sets we have confirmed that the NLO spectrum obtained from the sum of the spectra individually obtained with the pions, kaons and protons FFs is indeed equal to the one obtained with the non-identified charged hadron FFs.

role. Although the inclusive hadron FFs used in our NLO calculations contain *all* pion, kaons and (anti)protons issuing from light- as well as heavy-quark fragmentation, charm and bottom hadrons decay also into charged leptons[3] which are not included in INCNLO. Thus as a independent theoretical check, we have computed the inclusive yield of *all* charged particles with the PYTHIA MC (v6.420) [41] with the D6T [48] tuning[4] in the "minimum bias" and QCD-jets modes (`MSEL = 1` with low-p_T production, `ISUB = 95`, switched on to correctly simulate the low-p_T region). The chosen processes produce not only light-quarks and gluons but also heavy-quarks[5] including flavour excitation, $Qg \to Qg$, and gluon splitting, $g \to Q\bar{Q}$.

To obtain enough statistics at high-p_T, we have run with up to 12 different ranges for the minimum and maximum parton momenta in the 2→2 scatterings ($\hat{p}_T = 0 - 10, 10 - 15, 15 - 20, 20 - 50$ GeV/c,... and $\hat{p}_T > 470$ GeV/c) weighted by their corresponding cross sections. We have then explicitly separated the contributions coming from the fragmentation of high-p_T light-flavours (u, d, s and gluon) from those coming from charm and bottom quarks. As done in CDF, we take all charged particles exactly as defined in their analysis[6] (i.e. all primary particles with mean lifetimes $\tau > 0.3\ 10^{-10}$ s and the decay products of those particles with shorter τ). The results of our studies are shown in figure 3. The inclusive charged products of c-quark and b-quark fragmentation represent a very small (less than 5%) fraction of the total yield of particles measured at high-p_T by CDF.

A second possibility that we have explored is whether the charged products of real and virtual vector-boson ($\gamma^{(\star)}$, $W^{\pm}$, and Z^0) production — either single-inclusive or in association with a jet — which start to play a role at increasing transverse momenta, could partially account for the data-theory discrepancy. We have run prompt photon production in PYTHIA including the Born-level γ-jet Compton and annihilation diagrams (`ISUB = 29,14` respectively). The $W^{\pm}$, Z^0 and DY production (`ISUB = 1,2,15,16,30,31`), includes single-inclusive ($2 \to 1$) as well as double-inclusive ($2 \to 2$) $W^{\pm}$-,Z^0-,DY-jet channels with $\hat{p}_T > 20$ GeV/c. The $W^{\pm}$ and Z^0 contributions produce a (local) Jacobian peak in the charged-particle p_T distribution at about half the vector-boson mass, $p_T \approx 40$ GeV/c. All those contributions, shown added up in figure 3, increase the charged particle yield by up to 10% in the range above $p_T \approx 40$ GeV/c. This number is consistent with a simple order of magnitude estimate based on the ratio of electroweak and strong coupling constants (valid when $p_T \gg M_W/2$), $(\alpha_{\rm EW}/\alpha_s)^2 = (0.034/0.12)^2 = \mathcal{O}\left(10^{-1}\right)$. Clearly, those processes contribute little to the total yield of charged particles and therefore cannot justify the observed discrepancy between data and theory.

---

[3]As a cross check, we have confirmed that the PYTHIA spectrum of single leptons from c and b production agrees relatively well (within a factor of two) with more involved fixed-order NLL calculations [46, 47].

[4]Tune D6T uses the CTEQ6LL PDF and describes the underlying event and the Drell-Yan data at Tevatron.

[5]PYTHIA settings: `PARP(91)=2.1` GeV/c (intrinsic k_T), `PMAS(4,1)=1.5` GeV/c^2 (m_c mass), `PMAS(5,1)=4.8` GeV/c^2 (m_b mass), `MSTP(33)=1` (K-factor). Alternative running of *standalone* heavy-quark production (with `MSEL = 4` and 5) would require K-factors of $2 - 4$ in order to reproduce the heavy flavour p_T spectra measured at various colliders [49].
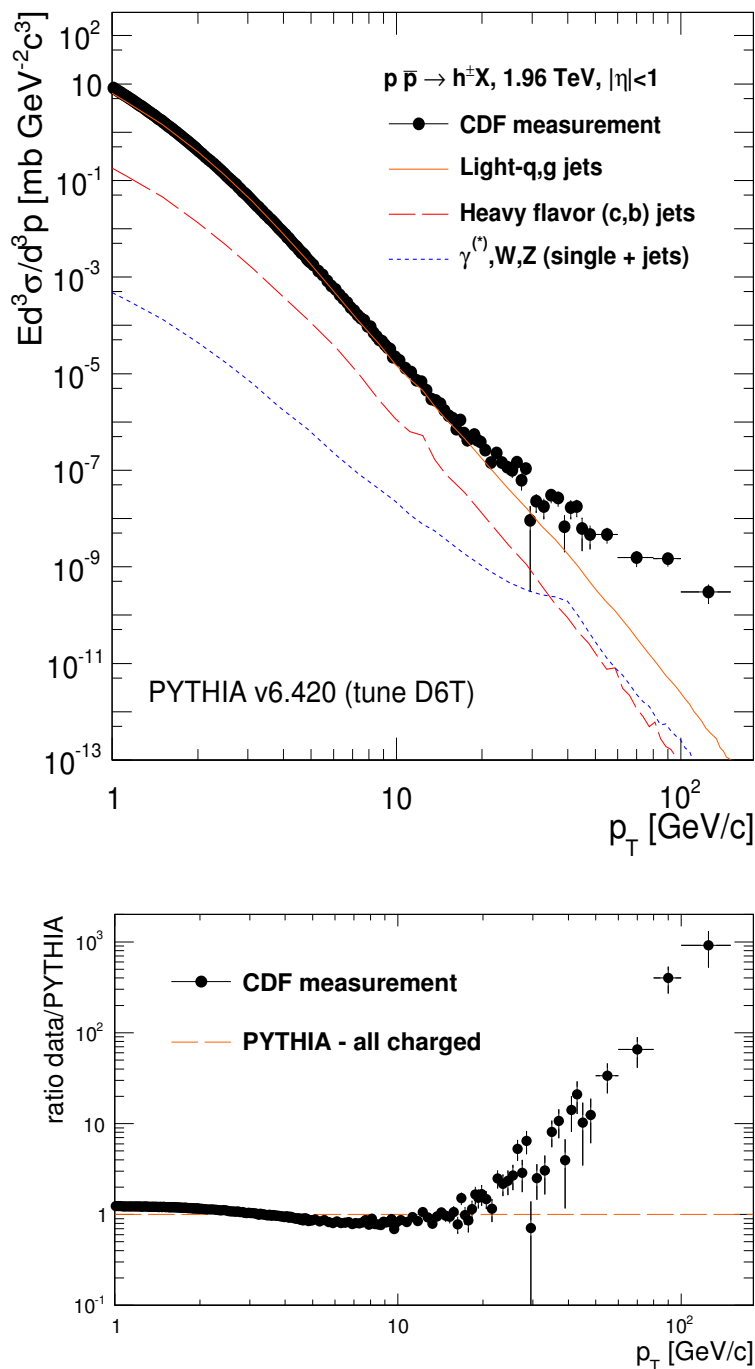
[6]PYTHIA settings: `MSTJ(22)= 2, PARJ(71)=10`.

Figure 3. Top: Comparison of the CDF data (symbols) to PYTHIA (v6.420, D6T tuning) p_T distribution of charged particles in p-$\bar{p}$ collisions at $\sqrt{s} = 1.96\,\text{TeV}$ coming from the fragmentation of (i) light-quarks and gluons and (ii) heavy-quarks, and (iii) from processes involving the production of vector bosons ($\gamma^{(\star)}$, $W^{\pm}$, Z^0). Bottom: Ratio of the CDF data to the sum of all PYTHIA charged particle contributions.
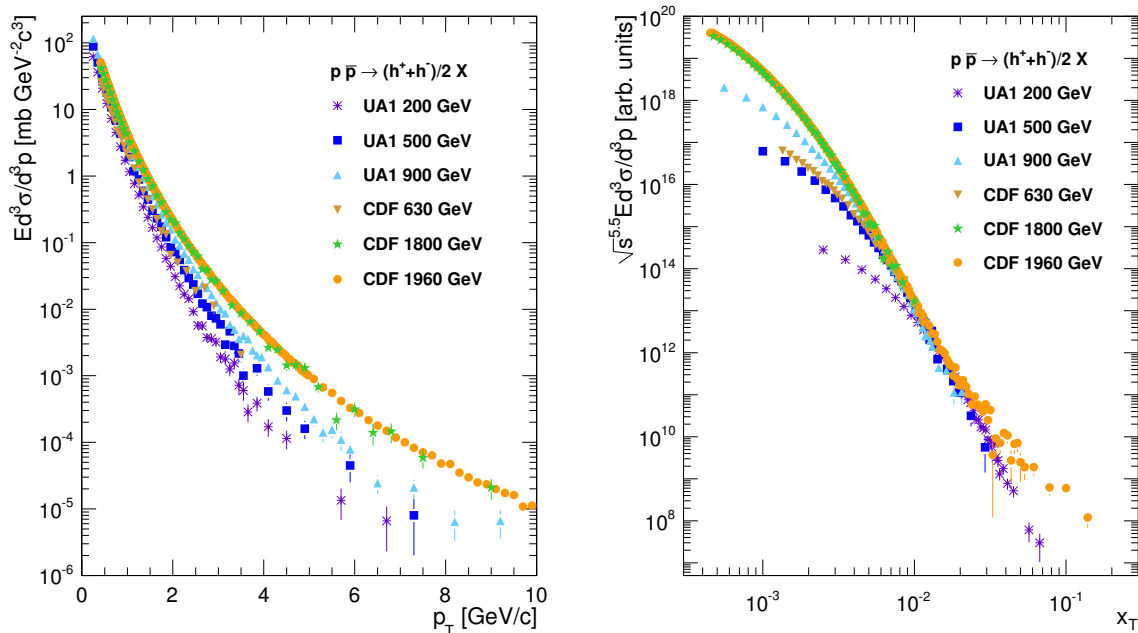
Figure 4. Compiled charged particle cross-sections measured in p-$\bar{p}$ collisions at five different c.m. energies from 0.2 TeV to 1.96 TeV plotted as a function of p_T (left) and as a function of x_T (right) scaled with an effective common exponent of $n = 5.5$ (see text).

3.3 Data versus x_T-scaling

A robust pQCD prediction for hard processes $A\ B \to C\ X$ in hadronic collisions is the power-law scaling of the inclusive invariant cross section,

$$E\, d^3\sigma/d^3p = F(x_T)/p_T^{n(x_T,\sqrt{s})} = F'(x_T)/\sqrt{s}^{\,n(x_T,\sqrt{s})} \ . \tag{3.1}$$

In the original parton model the power-law fall-off of the spectrum is simply $n = 4$ since the underlying $2 \to 2$ subprocess amplitude for point-like partons is scale invariant. In QCD, small scaling violations appear due to the running of α_S and the evolution of PDFs and FFs. At midrapidity and at fixed $p_T = 10$ GeV$/c$, the power-law exponent computed at NLO accuracy increases slowly from $n \simeq 5$ at small values of x_T ($x_T = 10^{-2}$) up to $n \simeq 6$ at $x_T = 0.5$, with a very small dependence on the specific hadron species [50].

Except for the latest CDF data, the theoretical expectation, eq. (3.1), is indeed well fulfilled by the experimental charged particle spectra measured so far in p-$\bar{p}$ collisions[7] at different centre-of-mass energies at the CERN Sp$\bar{p}$S ($\sqrt{s} = 0.2$, 0.5, 0.9 TeV) [17] and Tevatron ($\sqrt{s} = 0.63$, 1.8, 1.96 TeV) [18, 20] colliders. All the p_T spectra feature power-law behaviours above $p_T \approx 2$ GeV$/c$ (the higher the c.m. energy the smaller the exponent of the fall-off, see figure 4 left). Following the expectation eq. (3.1), in order to extract a common n value from these different data sets, the measurements are plotted as a function

---

[7]A factor of $1/2$ is applied hereafter to the CDF Run II spectrum as they measured $(h^+ + h^-)$ instead of the average $0.5 \times (h^+ + h^-)$ for all other measurements.

of x_T, multiplied by $\sqrt{s}^n$ and fitted with the following 3-parameter functional form

$$\sqrt{s}^n \frac{E \mathrm{d}^3\sigma}{\mathrm{d}^3 p}\bigg|_{y=0} = p_0 \cdot [1 + (x_T/p_1)]^{p_2} \ . \tag{3.2}$$

In the data fitting, a minimum p_T of 2 GeV/c is applied to exclude the region where soft particle production (which does not follow x_T-scaling) is dominant, which is consistent with what is used in [50]. We also exclude the CDF Run-II data from the global fit since, as we see *a posteriori*, there is no possibility to get an agreement with the lower energy measurements. With the obtained $\{p_i\}$-parameters, using $n_{\mathrm{NLO}} \approx 5$ as a guidance, the exponent n is varied from 4 to 7 in incremental steps in order to minimize the following χ^2 function with MINUIT [51]

$$\chi^2(n, \{p_i\}) = \sum_{j=1}^{n_{dat}} \left[\frac{\frac{E \mathrm{d}^3\sigma}{\mathrm{d}^3 p}\big|_{y=0} - \left(\frac{p_0 \cdot [1+(x_T/p_1)]^{p_2}}{\sqrt{s}^n} \right)}{\sigma_j} \right]^2 \ , \tag{3.3}$$

where σ_j are the quadratic sum of the statistical and systematic experimental uncertainties. In figure 4 (right) we show the experimental charged particle spectra scaled by $\sqrt{s}^n$ as a function of x_T with the best value of n obtained from the fit, $n = 5.5$. We note that all measurements spanning a range of one order-of-magnitude in centre-of-mass energies follow a universal curve after rescaling up to the highest $x_T \sim 0.03$ measured at lower energy. A deviation of the CDF measurement at $\sqrt{s} = 1.96$ TeV from the trend established by the lower $\sqrt{s}$ measurements is prominent above $x_T \sim 0.03$ ($p_T \sim 30$ GeV/c).

In order to better assess the amount of deviation of the CDF data to the x_T-scaling expectation we show in figure 5 (top) the x_T-scaled fit obtained from all lower-energy data extrapolated to an expected p_T spectrum at $\sqrt{s} = 1.96$ TeV compared with the CDF Run II measurement and with the PYTHIA prediction shown in figure 3. As observed before, beyond $p_T \approx 20$ GeV/c the latest CDF data clearly fail to follow the x_T-scaling expectation fulfilled by the rest of charged hadron measurements.

3.4 Discussion

The fact that no combination of PDF, FF and/or theoretical scales in the NLO calculations is able to reproduce the Tevatron experimental data above $p_T \approx 20$ GeV/c by such a large factor is totally unexpected. Indeed, similar calculations based on FASTNLO/NLOJET++ [52, 53], reproduce perfectly well the inclusive jet spectrum measured in p-$\bar{p}$ collisions at $\sqrt{s} = 1.96$ TeV in the range $p_T^{jet} \approx 50 - 600$ GeV/c. The shape and magnitude of the CDF jet measurement is well reproduced using CTEQ6.1M PDFs and renormalization and factorization scales[8] set to $\mu_R = \mu_F = p_T^{jet}/2$ [54]. Likewise, the D∅ jet measurement agrees well with the same NLO predictions with CTEQ6.5M parton densities and $\mu_R = \mu_F = p_T^{jet}$ scales [55]. Variations of PDF and/or scales in the jet calculations, result in differences typically of order 10% – 15% for both measurements [54, 55].

---

[8]Note that in the inclusive jet calculation there is one scale less, the fragmentation one μ_F.
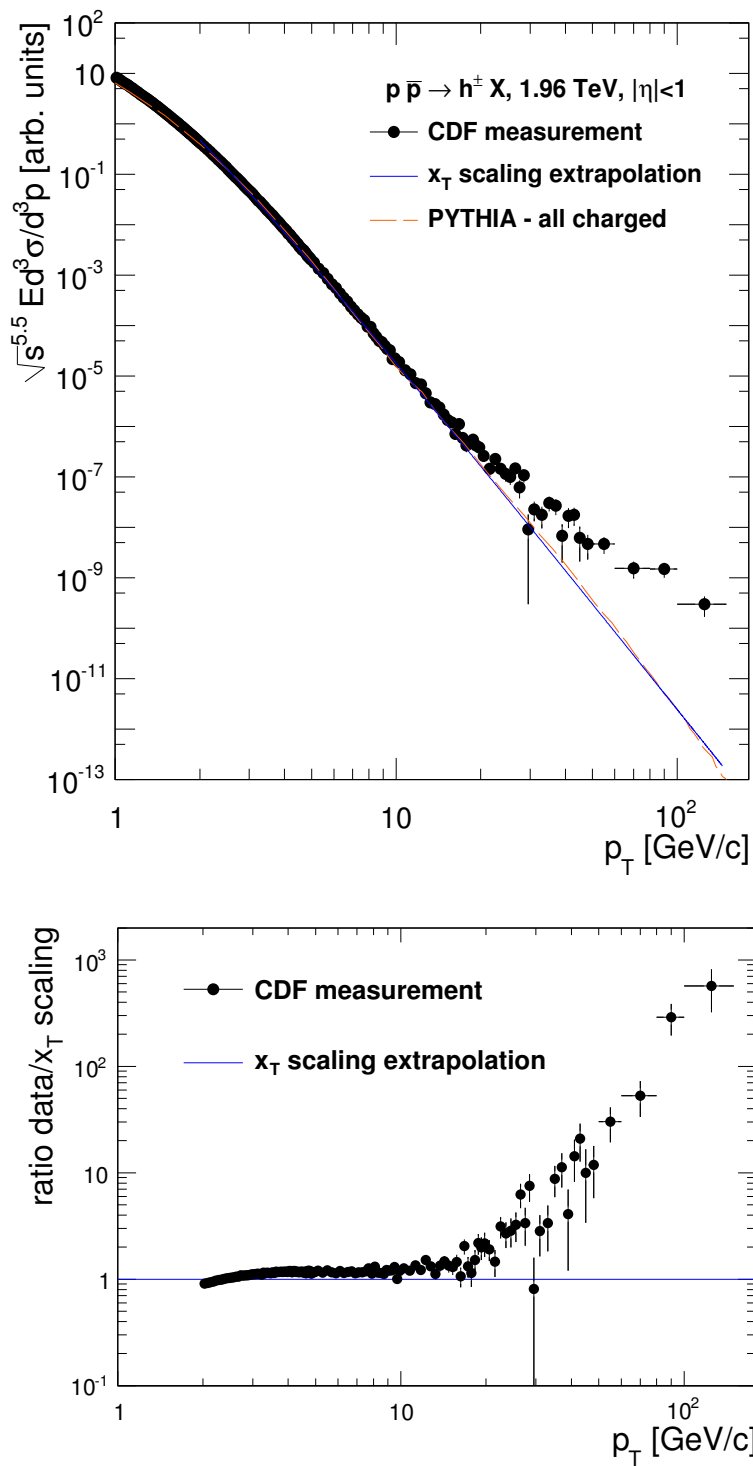
Figure 5. Top: Inclusive CDF Run-II charged hadron spectrum (filled circles) compared to the x_T-scaled extrapolation of lower energy p-$\bar{p}$ data (blue solid line), as well as to the total PYTHIA prediction (dashed red line) of figure 3. Bottom: Corresponding ratio of CDF data over x_T-scaling expectation.

Given the agreement between the jet data and the fixed-order calculations,[9] it is somehow difficult to conceive a strong disagreement in the hadron production channel since the single high-p_T charged particle spectrum is dominated by leading hadrons carrying out a large fraction, $\langle z \rangle \approx 0.6\text{-}0.7$, of the parent parton energy. Quite naively, the distribution of charged hadrons above $p_T \sim \langle z \rangle \ p_T^{jet} \gtrsim 30 \text{ GeV}/c$ should be also perfectly consistent with the theoretical predictions within the additional uncertainty introduced by the fragmentation functions which is at most of the order $\pm 25\%$ as seen in figure 2 (bottom). Let us give a rough estimate of the expected invariant hadron production cross section based on the jet data. At leading order accuracy and assuming that one partonic channel dominates jet and hadron production (e.g. $u\bar{u} \to u\bar{u}$ scattering at large x_T), the hadron production cross section eq. (2.1) is roughly given by

$$\frac{\mathrm{d}^3\sigma^h}{\mathrm{d}^3p}(p_T) \sim \frac{\mathrm{d}^3\sigma^{jet}}{\mathrm{d}^3p}\left(\frac{p_T}{z}\right) \times D_u^{h^++h^-}(z,p_T) \times \Delta z \simeq 10^{-2} \times \frac{\mathrm{d}^3\sigma^{jet}}{\mathrm{d}^3p}\left(\frac{p_T}{z}\right)$$

with $z \simeq 0.7$, the typical range $\Delta z \simeq 10^{-1}$ which contributes to the hadron production cross section, and $D_u^{h^++h^-}(z,p_T) \simeq 10^{-1}$ the u-quark-to-hadron FF (see e.g. [57]). Using the DØ jet measurement of $\mathrm{d}^2\sigma^{jet}/\mathrm{d}p_T\mathrm{d}y \simeq 200 \text{ pb}/(\text{GeV}/c)$ at $p_T = 100/z \simeq 140 \text{ GeV}/c$ and $|y| < 1$ [55], one gets for the hadron production cross section a value of $\mathrm{d}^3\sigma^h/\mathrm{d}^3p \simeq 2 \times 10^{-12} \text{ mb}/(\text{GeV}/c)^2$ which is the right order of magnitude estimate expected in QCD (see the LO PYTHIA curve in figure 3). The inconsistency between jet and the CDF large-p_T hadron spectrum is also discussed in detail in [59, 60].

Of course the above argument relies on the factorization assumption that large-p_T hadron production can be expressed as a convolution of hard matrix elements with parton-to-hadron fragmentation functions. Should the FFs – mostly based on fits of e^+e^- data – be non-universal one could imagine that the recent CDF measurement actually reflects dramatic modifications of fragmentation functions in hadronic collisions. This however seems unlikely given the success of the DSS [35] and AKK08 [36] global fits of fragmentation functions which consistently use e^+e^- data together with RHIC measurements in p-p collisions at $\sqrt{s} = 200 \text{ GeV}$. It is in particular unclear how possible factorization breaking effects could enhance hadron production cross sections by up to 3 orders of magnitude at transverse momenta as large as $p_T = 150 \text{ GeV}/c$.

There exist even more general arguments why the large-p_T CDF data cannot be understood as coming from hadron production in perturbative QCD. As discussed in the previous section (section 3.3), the recent CDF spectrum departs from the x_T-scaling behaviour observed in the lower-energy data which can all be described assuming a scaling exponent $n \simeq 5.5$. We find on the contrary that the scaling exponent obtained from the comparison of the large-p_T CDF measurement with the UA1 data at $\sqrt{s} = 200 \text{ GeV}$ is roughly[10] $n \simeq 4\text{-}4.7$. This value is extremely close to what is expected in the conformal limit ($n = 4$), i.e. assuming no scaling violations at all in QCD. It is in particular smaller than the exponents

---

[9] Prompt photon data at the Tevatron are also very well reproduced at large p_T by NLO pQCD calculations [56].

[10] The precise value is difficult to obtain since the x_T-spectra at the two c.m. energies have a different slope, already indicating a non-conventional behaviour in one of the two data sets.

expected for jet and prompt photon production [50], despite the fact that scaling violations are expected to be stronger in the hadron production channel because of the additional fragmentation process. What is more, the scaling exponent n obtained at fixed x_T reflects the p_T-dependence of the hard partonic cross section $\hat{\sigma} \sim p_T^{-n}$. Because of the fast variation of the parton densities with x_T, the p_T-slope, α, of the invariant production cross section at fixed $\sqrt{s}$ is expected to be somehow larger than the scale dependence of the partonic cross section, i.e. $\alpha > n$. Surprisingly the value α obtained from a fit of CDF data alone above $p_T = 22$ GeV/c is as small as $\alpha \simeq 3.9$, that is *smaller* than the combined UA1-CDF scaling exponent $n \simeq$ 4-4.7 (and even lower than the smallest scaling exponent $n = 4$!). This clearly indicates that it is not possible to describe the Run-II CDF measurement as coming from hadron production in perturbative QCD. Hence factorization breaking effects in the fragmentation channel cannot be at the origin of the present discrepancy between data and NLO theory.

We conclude from this section that the facts that (i) the NLO calculations largely fail to reproduce the measured single-hadron spectrum at large p_T while reproducing well the single jet p_T-differential cross sections, and (ii) that the measurement violates simple phenomenological expectations such as x_T-scaling confirmed empirically in all hadronic collisions so far, point to a possible experimental problem in the data above $p_T \approx 20$ GeV/c – or from unknown sources of charged particles – rather than from a sudden breakdown of QCD perturbation theory in the hadron production channel.

After we finished this work, other analyses appeared [58–61] that point out to the same discrepancy between the CDF data [20] and NLO calculations. In [58], Albino, Kniehl and Krämer point out the disagreement between data and NLO theory and question the validity of factorization theorems for large-p_T hadron production, a possibility which we exclude (see discussion above). In [59] it is shown on general grounds that the spectrum measured by CDF is inconsistent with existing Tevatron data on the inclusive jet production cross section and the distribution of hadrons inside jets (a similar argument is given in [60]); this observation allows the authors to exclude, as well, the breakdown of factorization as a possible explanation of the data. They also conclude that new physics scenarios explaining the CDF excess are unlikely, yet they cannot be fully eliminated. Finally, it has been claimed in [61] that weak boson decays into hadrons might explain the CDF data. This possibility is however excluded as shown in section 3.2, either from the detailed PYTHIA calculations or from the order of magnitude estimate.[11]

4 Inclusive charged hadron spectra at the LHC

In this last section of the paper we present first the INCNLO predictions for the charged hadron p_T-differential cross sections at mid-rapidity ($|\eta| < 1$) in p-p collisions in the range of

---

[11]We believe that the calculations in [61] is incorrect partly because of the use of fragmentation functions which are two orders of magnitude larger than the usual fits from e^+e^- data, at large z. We also note that the Jacobian peak in the p_T-spectrum is located at $\sim m_W$ instead of $\sim m_W/2$. Finally it is difficult to conceive why the invariant cross section scales as $\sim s/p_T^6$ instead of conventional behaviour $\sim 1/p_T^4$ (we thank S. Brodsky for pointing this out), which might lead to another two order of magnitude, $\mathcal{O}\left(s/p_T^2\right)$, overestimate in [61].
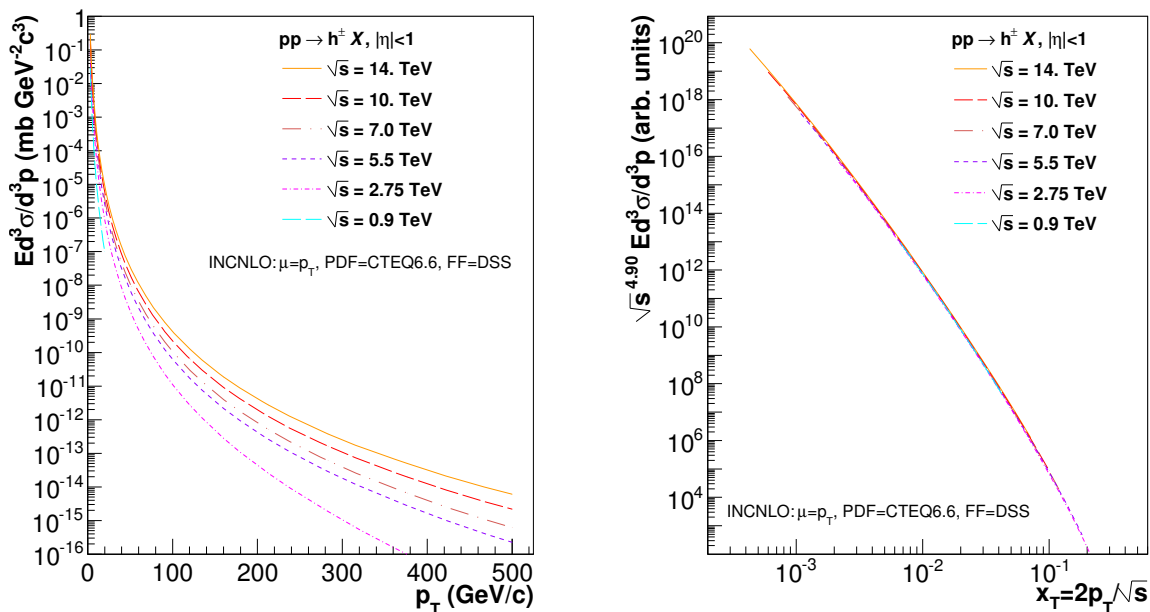
Figure 6. Charged hadron spectra in p-p collisions at $\sqrt{s} = $ 0.9, 2.76, 5.5, 7, 10 and 14 TeV predicted by NLO pQCD calculations with CTEQ6.6 parton distribution functions, DSS fragmentation functions, and scales set to $\mu = p_T$: p_T-differential (left) and x_T-scaled with exponent $n = 4.9$ (right).

CERN LHC energies ($\sqrt{s} = 0.9$–14 TeV) including their expected theoretical uncertainties. Second, we discuss two interpolation methods, based on pQCD-ratios and x_T-scaling, that can be used to obtain a baseline charged hadron p-p spectrum at intermediate LHC energies ($\sqrt{s} = $ 2.76, 5.5 TeV) needed to compare against similar measurements to be carried out in Pb-Pb collisions.

4.1 INCNLO **predictions**

Figure 6 (left) shows the INCNLO p_T-differential cross sections in $pp \rightarrow h^{\pm}X$ at six different c.m. energies (expected to be) reached at the LHC at various stages of the collider programme. The spectra have been obtained with CTEQ6.6 PDFs, DSS FFs and theoretical scales set to $\mu = p_T$. Whereas at p_T below about 10 GeV/c all calculations converge, with increasing c.m. energies (and thus phase-space for hard parton-parton scatterings), the spectra become increasingly flatter. For example, the charged hadron yield at $p_T \approx 100$ GeV/c, increases by a factor of 10 between $\sqrt{s} = 2.76$ TeV and $\sqrt{s} = 7$ TeV and yet by another factor of 5 between the latter and the top LHC energy of 14 TeV. As shown in figure 6 (right), for this particular choice of scales/PDFs/FFs, a common power-law exponent of $n = 4.9$ allows one to scale all NLO spectra in the range $\sqrt{s} = 0.9 - 14$ TeV to a universal curve, using the x_T prescription given by eq. (3.1). This value is slightly smaller than what has been obtained in section 3.3 from Tevatron and Sp$\bar{\text{p}}$S measurements ($n = 5.5$), indicating as expected smaller scaling violations at larger c.m. energy [50].

To assess the uncertainties linked to the choice of PDFs, FFs and scales μ in the domain of energies covered by the LHC, we have computed $pp \rightarrow h^{\pm} X$ at a fixed $\sqrt{s} = 7$ TeV
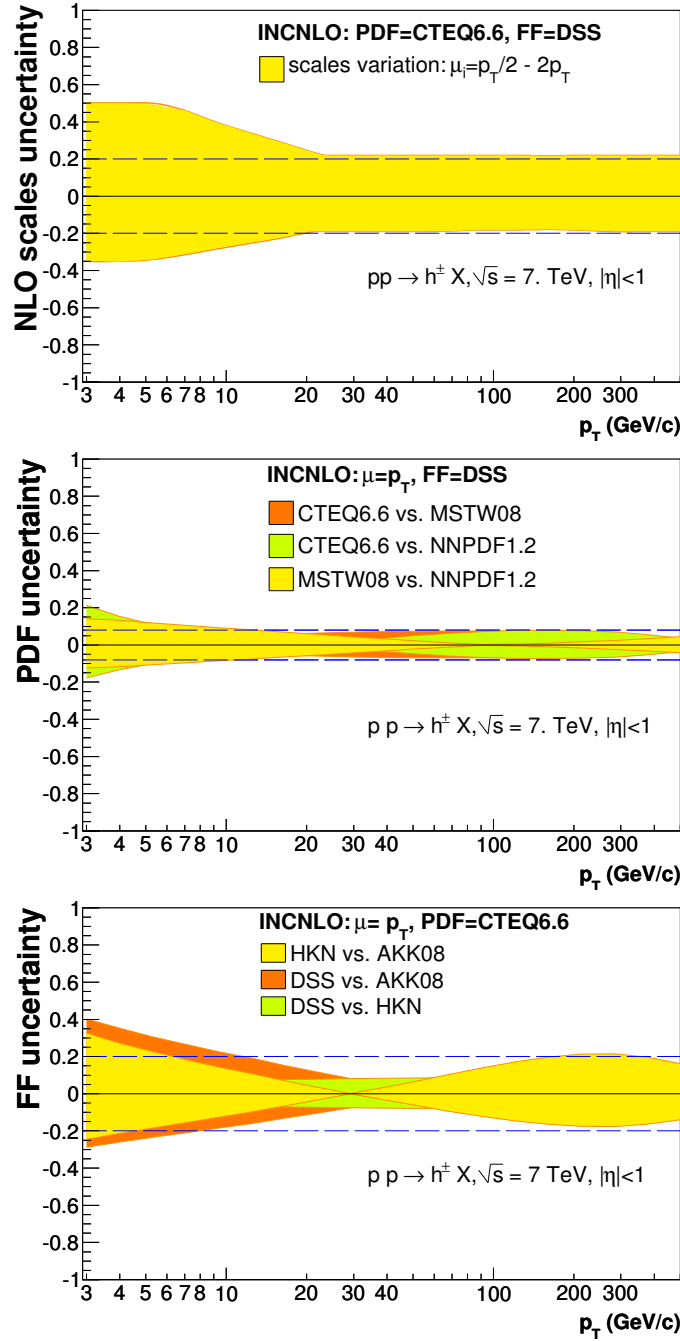
Figure 7. Fractional differences between the INCNLO charged hadron spectra in p-p at $\sqrt{s} = 7\,\text{TeV}$ for varying scales μ_i, PDF and FF. Top: Scale uncertainty obtained for fixed PDF (CTEQ6.6) and FF (DSS) varying all three scales within $\mu_i = p_T/2 - 2p_T$ (the dashed lines indicate a $\pm 20\%$ uncertainty). Middle: PDF uncertainty obtained for fixed $\mu = p_T$ and FF (DSS) with three PDFs: CTEQ6.6, MSTW08, NNPDF1.2 (the dashed lines indicate $\pm 8\%$ differences). Bottom: FF uncertainty obtained for fixed scales ($\mu = p_T$) and PDF (CTEQ6.6) with three FFs: AKK08, DSS, HKNS (the dashed lines represent $\pm 20\%$).

for various combinations of the theoretical ingredients as done for the Tevatron prediction (see section 3.1). Figure 7 (top) shows that the scale uncertainty is smaller ($\pm 20\%$ above $p_{_T} \approx 10\,\mathrm{GeV}/c$) than found at lower (Tevatron) energies (see figure 2 top). The middle plot of figure 7 shows that the uncertainty linked to the PDF choice is also slightly smaller than found at Tevatron, of the order of $\pm 8\%$. Finally, the bottom panel shows that the fractional FF uncertainty is at most of $\pm 20\%$ above $p_{_T} \approx 10\,\mathrm{GeV}/c$, whereas below that transverse momentum the uncertainties increase up to $\pm 40\%$. In the range $p_{_T} \approx 30$–$60\,\mathrm{GeV}/c$ the FF choice has uncertainties of only 10 percent. Those results point again to a somehow smaller FF uncertainty than found at Tevatron (see figure 2 bottom). A simple quadrature addition of the fractional uncertainties linked to the scales, PDF and FF choices results in a total theoretical uncertainty of around $\pm 35\%$ for the NLO single inclusive charged hadron spectrum in p-p collisions at LHC energies.

4.2 Interpolation of measured charged-hadron spectra at $\sqrt{s}$=5.5 TeV

One of the assets of the successful RHIC physics program has been the ability to study the production of hard processes in p-p and nucleus-nucleus (A-A) collisions at the *same* centre-of-mass energy. At the LHC, protons and ions have to travel in the same magnetic lattice[12] i.e. the two beams are required to have the same charge-to-mass ratio Z/A. This limits the beam momentum of a given species to $p = 7\,\mathrm{TeV} \times Z/A$ for the nominal 8.3 T dipole bending field. The nominal nucleon-nucleon c.m. energy for Pb-Pb collisions at the LHC is thus $\sqrt{s_{_{NN}}} = 5.5\,\mathrm{TeV}$ for lead ions with $A = 208$ and $Z = 82$. Since the maximum c.m. energy in the first LHC p-p runs is half of the nominal value, $\sqrt{s} = 7\,\mathrm{TeV}$ in lieu of $\sqrt{s} = 14\,\mathrm{TeV}$, the first Pb-Pb runs are actually expected at a maximum $\sqrt{s_{_{NN}}} = 2.76\,\mathrm{TeV}$. In order to correctly normalize the yields measured in Pb-Pb collisions at $\sqrt{s_{_{NN}}} = 2.76, 5.5\,\mathrm{TeV}$, it will be crucial to get reliable estimates of the corresponding cross sections in p-p collisions at the same c.m. energy. Ideally the predictions in p-p collisions should take advantage of the data accumulated at the LHC at nearby energies and be obtained with the smallest model-dependence possible to avoid any theoretical prejudice. In the following we present two methods for rescaling experimental p-p charged hadron spectra, measured at different c.m. energies than those expected for heavy-ion collisions, based respectively on pQCD yield ratios and $x_{_T}$-scaling.

4.2.1 Centre-of-mass energy rescaling

As seen in the previous section, at a given c.m. energy there are combined uncertainties of the order of $\pm 35\%$ in the NLO predictions for the *absolute* $p_{_T}$-differential cross sections of charged hadrons at LHC energies. Most of these uncertainties — in particular the largest scale dependence — however cancel out when taking *ratios* of the predicted perturbative yields at different, yet close, c.m. energies. One can, thus, rescale the p-p spectrum measured at a given $\sqrt{s} = X\,\mathrm{TeV}$ (say, 7 TeV) to a $\sqrt{s} = 2.76, 5.5\,\mathrm{TeV}$ reference value with

---

[12]The magnetic rigidity is defined as $p/Z = B\,r$ for an ion with momentum p and charge Z that would have a bending radius r in a magnetic field B.
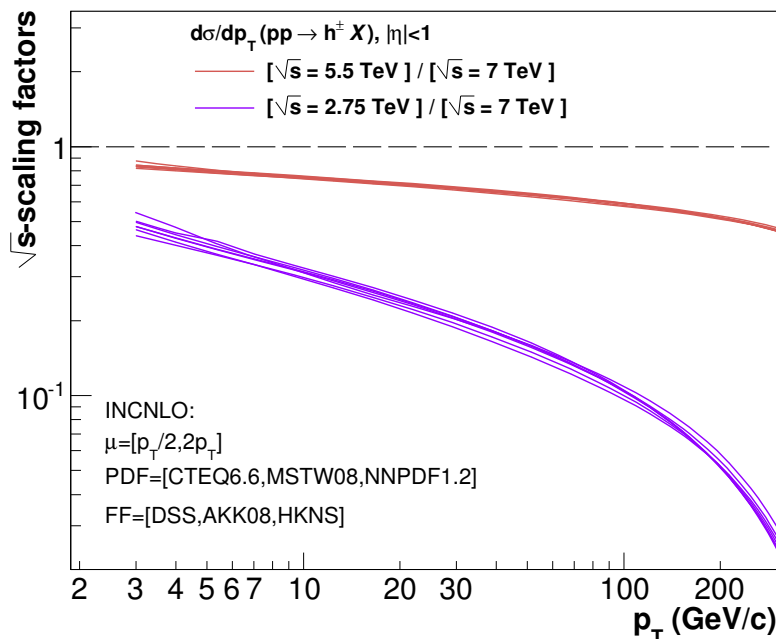
Figure 8. Rescaling factors of the p_T-differential charged hadron cross-sections in p-p at $\sqrt{s} = 7\,\text{TeV}$ down to lower $\sqrt{s} = 2.76$, $5.5\,\text{TeV}$ values, obtained from the ratio of the corresponding NLO calculations, eq. (4.1). The various curves show the small residual differences arising from different scale/PDF/FF choices.

a simple prescription:

$$\frac{\mathrm{d}\sigma_{\text{ref}}\ (\sqrt{s} = 2.76, 5.5\ \text{TeV})}{\mathrm{d}p_T} = \left(\frac{\mathrm{d}\sigma_{\text{NLO}}/\mathrm{d}p_T\ (\sqrt{s} = 2.76, 5.5\ \text{TeV})}{\mathrm{d}\sigma_{\text{NLO}}/\mathrm{d}p_T\ (\sqrt{s} = X\ \text{TeV})}\right) \times \frac{\mathrm{d}\sigma_{\text{exp}}\ (\sqrt{s} = X\ \text{TeV})}{\mathrm{d}p_T}. \tag{4.1}$$

As an example, we plot in figure 8 the scaling factors as a function of p_T obtained from the ratios of 2.76-TeV/7-TeV and 5.5-TeV/7-TeV pQCD yields. They have been obtained with up to 14 combinations of the different theoretical ingredients (scales, PDFs and FFs). The important scale dependence (figure 7, top) largely cancels out and only residual differences arise from the slightly different parton x and hadron z momentum fractions probed at different energies (of course, the closer the c.m. energies the smaller the uncertainty in the yield ratios). The maximum theoretical uncertainties of the rescaling factors amount to a small $\pm 5\%$ (resp. $\pm 12\%$) for $\sqrt{s} = 5.5\,\text{TeV}$ (resp. $2.76\,\text{TeV}$), which will be likely below the expected uncertainties in the 7-TeV p-p experimental spectrum alone.

4.2.2 x_T-scaling

In this last section, we suggest to use the x_T-scaling of particle production in high-energy scattering discussed in section 3.3 in order to predict the large-p_T hadron production cross sections in p-p collisions at $\sqrt{s} = 2.76$ and $5.5\,\text{TeV}$ from the interpolation of Tevatron ($\sqrt{s} = 1.96\,\text{TeV}$) and LHC ($\sqrt{s} = 7\,\text{TeV}$) data.

Assuming that eq. (3.1) holds from Tevatron to LHC,[13] it is straightforward to deduce the invariant cross section at a given $\sqrt{s}$ and x_T from previous measurements performed at Tevatron and LHC. Using the power-law interpolation,[14] eq. (3.1), the invariant cross section $\sigma^{\mathrm{inv}} \equiv E\, d^3\sigma/d^3p$ reads

$$\sigma^{\mathrm{inv}}(\sqrt{s}, x_T) = \sigma^{\mathrm{inv}}\left(\sqrt{s}, p_T = x_T \frac{\sqrt{s}}{2}\right) = \sigma^{\mathrm{inv}}(1.96~\mathrm{TeV}, x_T) \times \left[\frac{\sigma^{\mathrm{inv}}(7~\mathrm{TeV}, x_T)}{\sigma^{\mathrm{inv}}(1.96~\mathrm{TeV}, x_T)}\right]^{\alpha}$$
(4.2)

where we define $\alpha \equiv \ln(\sqrt{s}/1.96)/\ln(7/1.96)$. The relative uncertainty on the cross section at $\sqrt{s}$ resulting from the power-law interpolation from the data at 7 and 1.96 TeV is thus simply given by

$$\frac{\delta\sigma^{\mathrm{inv}}(\sqrt{s}, x_T)}{\sigma^{\mathrm{inv}}(\sqrt{s}, x_T)} = \sqrt{(1-\alpha)^2 \left(\frac{\delta\sigma^{\mathrm{inv}}(1.96~\mathrm{TeV}, x_T)}{\sigma^{\mathrm{inv}}(1.96~\mathrm{TeV}, x_T)}\right)^2 + \alpha^2 \left(\frac{\delta\sigma^{\mathrm{inv}}(7~\mathrm{TeV}, x_T)}{\sigma^{\mathrm{inv}}(7~\mathrm{TeV}, x_T)}\right)^2} \quad (4.3)$$

where $\delta\sigma^{\mathrm{inv}}(1.96~\mathrm{TeV}, x_T)$ and $\delta\sigma^{\mathrm{inv}}(7~\mathrm{TeV}, x_T)$ are the uncertainties of spectra measured at Tevatron and LHC, respectively. Let us suppose for simplicity that the experimental relative uncertainty $\delta\sigma^{\mathrm{inv}}/\sigma^{\mathrm{inv}}$ on the hadron spectrum is identical at Tevatron and LHC, thus the relative uncertainty on the interpolated cross section at $\sqrt{s}$ will be $\sqrt{\alpha^2 + (1-\alpha)^2} \times \delta\sigma/\sigma$, i.e. $0.83\, \delta\sigma^{\mathrm{inv}}/\sigma^{\mathrm{inv}}$ at both $\sqrt{s} = 2.76$ and 5.5 TeV. Therefore, if the measurements at Tevatron and LHC used for the interpolation are precise enough, this procedure would allow for predictions whose uncertainties become possibly smaller than the usual theoretical uncertainties of NLO QCD calculations. Note however that the uncertainty eq. (4.3) only reflects the propagation of errors in the power-law interpolation and does not account for the systematic uncertainty of the procedure currently used.

Since the invariant cross sections are compared at a given x_T, the p_T range reached at the lower (Tevatron) and upper (LHC) limits of the interpolation domain is crucial. The currently "reliable" Tevatron data extend up to $p_T \simeq 20$ GeV/c which allows for a prediction up to $p_T \simeq 30$ (60) GeV/c at $\sqrt{s} = 2.76$ (5.5) TeV. Conversely, the upper limit at $\sqrt{s} = 2.76$ (5.5) TeV is 40% (80%) of the highest p_T to be reached at $\sqrt{s} = 7$ TeV.

In order to check this procedure, the p_T-spectrum of mid-rapidity charged hadrons at $\sqrt{s} = 5.5$ TeV has been estimated from the PYTHIA spectra at $\sqrt{s} = 1.96$ and at 7 TeV using the interpolation eq. (4.2) with $\alpha = 0.81$, within the range $x_T \approx 2{\cdot}10^{-3}$–0.2. The result is plotted in figure 9 and compared to the direct PYTHIA calculation of the hadron spectrum at $\sqrt{s} = 5.5$ TeV. As it can be seen, the x_T- interpolated cross section reproduces nicely the MC result at $\sqrt{s} = 5.5$ TeV above $p_T \approx 5$ GeV/c.

---

[13]We note that the Tevatron data are measured in p–$\bar{p}$ collisions unlike the p-p collisions at the LHC. The differences between both systems on unidentified hadron production at midrapidity is very small (especially, far away from the valence quark region, i.e. for $x_T \ll 1$).

[14]Note that the exponent n depends in principle on p_T (and thus x_T) from the scaling violations in QCD and should approach $n = 4$ in the Bjorken limit. However this dependence is expected to be logarithmic and can be safely neglected in the p_T-range being considered here.
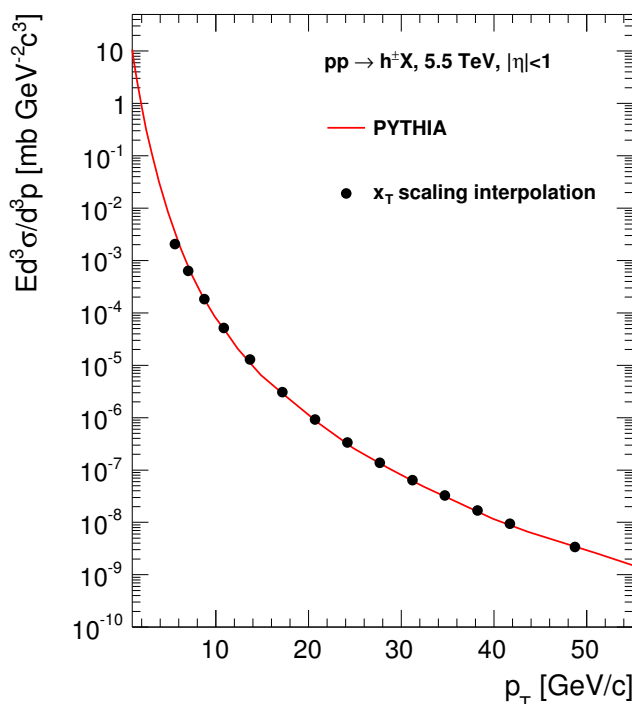
Figure 9. Comparison of the PYTHIA charged hadron spectrum in p-p collisions at $\sqrt{s} = 5.5\,\mathrm{TeV}$ to the x_T-scaling interpolation obtained via eq. (4.2) from the corresponding PYTHIA spectra at $\sqrt{s} = 1.96\,\mathrm{TeV}$ (p-$\bar{p}$) and 7 TeV (p-p).

5 Summary

We have compared the latest high-p_T charged particle spectrum measured by CDF in proton-antiproton collisions at $\sqrt{s} = 1.96\,\mathrm{TeV}$ to various perturbative QCD expectations based on next-to-leading-order calculations (INCNLO), parton-shower Monte Carlo (PYTHIA), and x_T-scaling respectively. The NLO calculations employ the latest sets of parton distribution functions (PDFs) and fragmentation functions (FFs). The Tevatron data can be well reproduced below $p_T \approx 20$ GeV/c for the choice of scales $\mu = 2p_T$, CTEQ6.6 parton densities, and AKK08 parton-to-hadron fragmentation functions. Above this p_T value, the CDF spectrum starts to rapidly deviate, by up to three orders of magnitude, from the predictions. The most important source of theoretical uncertainty, of order ±30%, is related to the choice of the factorization, fragmentation and normalization scales. The maximum uncertainties linked to the choice of the PDFs and FFs are ±10% and ±25% respectively. A conservative quadratic addition of all these differences results in a total ±40% uncertainty in the NLO calculations which cannot by any means explain the important data-theory disagreement above $p_T \approx 20$ GeV/c.

We have next determined with the PYTHIA MC the possible extra contributions of high-p_T charged particles, including leptons, coming from heavy-quark fragmentation as well as from real and virtual vector-boson production either single-inclusive or in association with

a jet. The addition of such processes, which amount to about an additional ten percent of the charged particle yield above $p_T \approx 40$ GeV/c, does not help to reduce the large data-theory deviation. The CDF spectrum also fails to fulfill simple x_T scaling expectations which are empirically confirmed by all other high-p_T hadron spectra measured so far in p-$\bar{p}$ collisions in the range $\sqrt{s} = 0.2$–1.8 TeV. Moreover, the power-law exponent of the CDF data above $x_T \approx 0.02$, is below the $n = 4$ limit expected from simple dimensional arguments for pure $2 \rightarrow 2$ parton scattering in QCD.

We conclude that the fact that the NLO calculations largely fail to reproduce the measured CDF single hadron spectrum at large p_T while simultaneously reproducing correctly the single jet p_T-differential cross sections, and that the measurement violates simple phenomenological expectations such as x_T-scaling, point to a possible experimental problem in the Tevatron data above $p_T \approx 20$ GeV/c (or to unknown sources of charged particles not considered here, a possibility disfavored in [59]).

The NLO predictions of charged hadron spectra at LHC energies $\sqrt{s} = 0.9$–14 TeV, have also been provided. Finally, we have proposed two simple interpolation procedures, based on a pQCD-rescaling and an x_T-scaling of (future) experimental p-p transverse momentum spectra, in order to obtain the nuclear modification factors of high-p_T charged hadron production in nucleus-nucleus collisions at intermediate ($\sqrt{s_{NN}} = 2.76$, 5.5 TeV) LHC energies.

Acknowledgments

References

[1] J.C. Collins, D.E. Soper and G. Sterman, *Factorization for short distance hadron-hadron scattering*, *Nucl. Phys.* **B 261** (1985) 104 [SPIRES].

[2] J.F. Owens, E. Reya and M. Gluck, *Detailed quantum chromodynamic predictions for high p_T processes*, *Phys. Rev.* **D 18** (1978) 1501 [SPIRES].

[3] F. Aversa, P. Chiappetta, M. Greco and J.P. Guillet, *QCD corrections to parton-parton scattering processes*, *Nucl. Phys.* **B 327** (1989) 105 [SPIRES].

[4] D. de Florian, *Next-to-leading order QCD corrections to one hadron production in polarized pp collisions at RHIC*, *Phys. Rev.* **D 67** (2003) 054004 [hep-ph/0210442] [SPIRES].

[5] B. Jäger, A. Schäfer, M. Stratmann and W. Vogelsang, *Next-to-leading order QCD corrections to high-p_T pion production in longitudinally polarized pp collisions*, *Phys. Rev.* **D 67** (2003) 054005 [hep-ph/0211007] [SPIRES].

[6] D. de Florian and W. Vogelsang, *Threshold resummation for the inclusive hadron cross-section in pp collisions*, *Phys. Rev.* **D 71** (2005) 114004 [`hep-ph/0501258`] [SPIRES].

[7] W. Vogelsang, private communication.

[8] D. de Florian, W. Vogelsang and F. Wagner, *Single-inclusive hadron production in polarized pp scattering at next-to-leading logarithmic accuracy*, *Phys. Rev.* **D 76** (2007) 094021 [`arXiv:0708.3060`] [SPIRES].

[9] PHENIX collaboration, S.S. Adler et al., *Measurement of transverse single-spin asymmetries for mid-rapidity production of neutral pions and charged hadrons in polarized $p + p$ collisions at $\sqrt{s} = 200\,GeV$*, *Phys. Rev. Lett.* **95** (2005) 202001 [`hep-ex/0507073`] [SPIRES].

[10] S. Albino, *The Hadronization of partons*, `arXiv:0810.4255` [SPIRES].

[11] F. Arleo, *(Medium-modified) fragmentation functions*, *Eur. Phys. J.* **C 61** (2009) 603 [`arXiv:0810.1193`] [SPIRES].

[12] D. d'Enterria and B. Betz, *High-p_T hadron suppression and jet quenching*, *Lect. Notes Phys.* **785** (2010) 285 [SPIRES].

[13] AMES-BOLOGNA-CERN-DORTMUND-HEIDELBERG-WARSAW collaboration, A. Breakstone et al., *Inclusive charged particle cross-sections in full phase space from proton proton interactions at ISR energies*, *Z. Phys.* **C 69** (1995) 55 [SPIRES].

[14] AXIAL FIELD SPECTROMETER collaboration, T. Akesson et al., *Large transverse momentum particle production in $\alpha\alpha$ and pp collisions at the CERN ISR*, *Nucl. Phys.* **B 209** (1982) 309 [SPIRES].

[15] STAR collaboration, J. Adams et al., *Transverse momentum and collision energy dependence of high p_T hadron suppression in $Au + Au$ collisions at ultrarelativistic energies*, *Phys. Rev. Lett.* **91** (2003) 172302 [`nucl-ex/0305015`] [SPIRES].

[16] BRAHMS collaboration, I. Arsene et al., *On the evolution of the nuclear modification factors with rapidity and centrality in $d + Au$ collisions at $s_{NN}^{1/2} = 200\,GeV$*, *Phys. Rev. Lett.* **93** (2004) 242303 [`nucl-ex/0403005`] [SPIRES].

[17] UA1 collaboration, C. Albajar et al., *A study of the general characteristics of $p\bar{p}$ collisions at $\sqrt{s} = 0.2\,TeV$ to $0.9\,TeV$*, *Nucl. Phys.* **B 335** (1990) 261 [SPIRES].

[18] CDF collaboration, F. Abe et al., *Transverse momentum distributions of charged particles produced in $\bar{p}p$ interactions at $\sqrt{s} = 630\,GeV$ and $1800\,GeV$*, *Phys. Rev. Lett.* **61** (1988) 1819 [SPIRES].

[19] CDF collaboration, D.E. Acosta et al., *Soft and hard interactions in $p\bar{p}$ collisions at $\sqrt{s} = 1800\,GeV$ and $630\,GeV$*, *Phys. Rev.* **D 65** (2002) 072005 [SPIRES].

[20] CDF collaboration, T. Aaltonen et al., *Measurement of particle production and inclusive differential cross sections in $p\bar{p}$ collisions at $\sqrt{s} = 1.96\,TeV$*, *Phys. Rev.* **D 79** (2009) 112005 [`arXiv:0904.1098`] [SPIRES].

[21] F. Sikler, *Towards measurement of charged hadron spectra in CMS*, `PoS(PoS(HIGH-pTLHC)011`.

[22] J.-P. Revol, *First measurements at LHC: early hadronic physics (soft + QCD) with ALICE, ATLAS, CMS, TOTEM and LHCb*, *Nucl. Phys. Proc. Suppl.* **177-178** (2008) 60 [SPIRES].

[23] ATLAS collaboration, W.H. Bell, *Minimum bias physics at the LHC with the ATLAS detector*, in 1$^{\text{st}}$ *International Workshop on Multiple Partonic Interactions at LHC*, October 27–31, Perugia, Italy (2008), ATL-PHYS-PROC-2009-051 [SPIRES].

[24] CMS collaboration, V. Khachatryan et al., *Transverse momentum and pseudorapidity distributions of charged hadrons in pp collisions at $\sqrt{(s)} = 0.9$ and 2.36 TeV*, *JHEP* **02** (2010) 041 [`arXiv:1002.0621`] [SPIRES].

[25] PHENIX collaboration, K. Adcox et al., *Formation of dense partonic matter in relativistic nucleus nucleus collisions at RHIC: Experimental evaluation by the PHENIX collaboration*, *Nucl. Phys.* **A 757** (2005) 184 [`nucl-ex/0410003`] [SPIRES].

[26] STAR collaboration, J. Adams et al., *Experimental and theoretical challenges in the search for the quark gluon plasma: The STAR collaboration's critical assessment of the evidence from RHIC collisions*, *Nucl. Phys.* **A 757** (2005) 102 [`nucl-ex/0501009`] [SPIRES].

[27] P. Aurenche, M. Fontannaz, J.P. Guillet, B.A. Kniehl and M. Werlen, *Large p_T inclusive π_0 cross-sections and next-to-leading-order QCD predictions*, *Eur. Phys. J.* **C 13** (2000) 347 [`hep-ph/9910252`] [SPIRES].

[28] P. Aurenche et al., *INCNLO-direct photon and inclusive hadron production code*, http://lappweb.in2p3.fr/lapth/PHOX_FAMILY/readme_inc.html.

[29] P. Aurenche, M. Fontannaz, J.P. Guillet, B.A. Kniehl and M. Werlen, *Large p_T inclusive π_0 cross-sections and next-to-leading-order QCD predictions*, *Eur. Phys. J.* **C 13** (2000) 347 [`hep-ph/9910252`] [SPIRES].

[30] P.M. Nadolsky et al., *Implications of CTEQ global analysis for collider observables*, *Phys. Rev.* **D 78** (2008) 013004 [`arXiv:0802.0007`] [SPIRES].

[31] A.D. Martin, W.J. Stirling, R.S. Thorne and G. Watt, *Parton distributions for the LHC*, *Eur. Phys. J.* **C 63** (2009) 189 [`arXiv:0901.0002`] [SPIRES].

[32] A.D. Martin, W.J. Stirling, R.S. Thorne and G. Watt, *Uncertainties on α_S in global PDF analyses and implications for predicted hadronic cross sections*, *Eur. Phys. J.* **C 64** (2009) 653 [`arXiv:0905.3531`] [SPIRES].

[33] NNPDF collaboration, R.D. Ball et al., *A determination of parton distributions with faithful uncertainty estimation*, *Nucl. Phys.* **B 809** (2009) 1 [*Erratum ibid.* **B 816** (2009) 293] [`arXiv:0808.1231`] [SPIRES].

[34] M.R. Whalley, D. Bourilkov and R.C. Group, *The Les Houches Accord PDFs (LHAPDF) and LHAGLUE*, http://hepforge.cedar.ac.uk/lhapdf/, `hep-ph/0508110` [SPIRES].

[35] D. de Florian, R. Sassot and M. Stratmann, *Global analysis of fragmentation functions for pions and kaons and their uncertainties*, *Phys. Rev.* **D 75** (2007) 114010 [`hep-ph/0703242`] [SPIRES].

[36] S. Albino, B.A. Kniehl and G. Kramer, *AKK update: improvements from new theoretical input and experimental data*, *Nucl. Phys.* **B 803** (2008) 42 [`arXiv:0803.2768`] [SPIRES].

[37] M. Hirai, S. Kumano, T.H. Nagai and K. Sudoh, *Determination of fragmentation functions and their uncertainties*, *Phys. Rev.* **D 75** (2007) 094009 [`hep-ph/0702250`] [SPIRES].

[38] G. Sterman, *Summation of large corrections to short distance hadronic cross-sections*, *Nucl. Phys.* **B 281** (1987) 310 [SPIRES].

[39] S. Catani and L. Trentadue, *Resummation of the QCD perturbative series for hard processes*, *Nucl. Phys.* **B 327** (1989) 323 [SPIRES].

[40] S. Catani and L. Trentadue, *Comment on QCD exponentiation at large x*, *Nucl. Phys.* **B 353** (1991) 183 [SPIRES].

[41] T. Sjöstrand, S. Mrenna and P.Z. Skands, *PYTHIA 6.4 physics and manual*, *JHEP* **05** (2006) 026 [`hep-ph/0603175`] [SPIRES].

[42] S.J. Brodsky and G.R. Farrar, *Scaling laws at large transverse momentum*, *Phys. Rev. Lett.* **31** (1973) 1153 [SPIRES].

[43] D.W. Sivers, S.J. Brodsky and R. Blankenbecler, *Large transverse momentum processes*, *Phys. Rept.* **23** (1976) 1 [SPIRES].

[44] R. Blankenbecler, S.J. Brodsky and J.F. Gunion, *The magnitude of large transverse momentum cross-sections*, *Phys. Rev.* **D 18** (1978) 900 [SPIRES].

[45] M.J. Tannenbaum, *Hard and soft physics at RHIC with implications for LHC*, arXiv:0904.4363 [SPIRES].

[46] M. Cacciari, S. Frixione, M.L. Mangano, P. Nason and G. Ridolfi, *QCD analysis of first b cross-section data at* 1.96 *TeV*, *JHEP* **07** (2004) 033 [hep-ph/0312132] [SPIRES].

[47] M. Cacciari, private communication.

[48] P. Bartalini, (ed.) et al., *Proceedings of the first international workshop on multiple partonic interactions at the LHC (MPI08)*, arXiv:1003.4220 [SPIRES].

[49] C. Lourenco and H.K. Wohri, *Heavy flavour hadro-production from fixed-target to collider energies*, *Phys. Rept.* **433** (2006) 127 [hep-ph/0609101] [SPIRES].

[50] F. Arleo, S.J. Brodsky, D.S. Hwang and A.M. Sickles, *Higher-twist dynamics in large transverse momentum hadron production*, arXiv:0911.4604 [SPIRES].

[51] F. James and M. Roos, *Minuit: a system for function minimization and analysis of the parameter errors and correlations*, *Comput. Phys. Commun.* **10** (1975) 343 [SPIRES].

[52] T. Kluge, K. Rabbertz and M. Wobisch, *Fast pQCD calculations for PDF fits*, hep-ph/0609285 [SPIRES].

[53] Z. Nagy, *Next-to-leading order calculation of three jet observables in hadron hadron collision*, *Phys. Rev.* **D 68** (2003) 094002 [hep-ph/0307268] [SPIRES].

[54] CDF collaboration, T. Aaltonen et al., *Measurement of the inclusive jet cross section at the Fermilab Tevatron p$\bar{p}$ collider using a cone-based jet algorithm*, *Phys. Rev.* **D 78** (2008) 052006 [*Erratum ibid.* **D 79** (2009) 119902] [arXiv:0807.2204] [SPIRES].

[55] D0 collaboration, V.M. Abazov et al., *Measurement of the inclusive jet cross-section in p$\bar{p}$ collisions at* $s^{(1/2)} = 1.96$ *TeV*, *Phys. Rev. Lett.* **101** (2008) 062001 [arXiv:0802.2400] [SPIRES].

[56] P. Aurenche, M. Fontannaz, J.-P. Guillet, E. Pilon and M. Werlen, *A New critical study of photon production in hadronic collisions*, *Phys. Rev.* **D 73** (2006) 094007 [hep-ph/0602133] [SPIRES].

[57] *Fragmentation function generator*, http://lappweb.in2p3.fr/lapth/generators.

[58] S. Albino, B.A. Kniehl and G. Kramer, *Factorization breaking in high-transverse-momentum charged-hadron production at the Tevatron?*, arXiv:1003.1854 [SPIRES].

[59] M. Cacciari, G.P. Salam and M.J. Strassler, *A note on the CDF high-p$_t$ charged particle excess*, arXiv:1003.3433 [SPIRES].

[60] A.S. Yoon, E. Wenger and G. Roland, *Convoluting jet spectra with fragmentation functions: a cross-check of the charged particle p$_T$ spectrum*, arXiv:1003.5928 [SPIRES].

[61] B.L. Ioffe, *Weak interaction contribution to the inclusive hadron-hadron scattering cross sections at high p$_T$*, arXiv:1005.1078 [SPIRES].